Journal of Hazardous Materials 166 (2009) 415–420

Contents lists available at ScienceDirect

Journal of Hazardous Materials

journal homepage: www.elsevier.com/locate/jhazmat

A new hybrid ion exchanger: Effect of system parameters on the adsorption of vanadium (V)

Bong-Yeol Yeom [a], Chang-Soo Lee [b], Taek-Sung Hwang [b,*]

[a] Nonwovens Cooperative Research Center, College of Textiles, North Carolina State University, Raleigh, NC 27695-8301, USA
[b] School of Applied Chemistry and Biological Engineering, College of Engineering, Chungnam National University, Daejeon 305-764, South Korea

ARTICLE INFO

Article history:
Received 23 May 2008
Received in revised form
30 September 2008
Accepted 14 November 2008
Available online 21 November 2008

Keywords:
PONF-g-GMA
Hybrid
Adsorption
Kinetics
Vanadium

ABSTRACT

The hybrid ion exchanger consisted of PONF-g-GMA anion fibrous exchanger and IRA-96 bead-type anion exchanger was developed by combining different types of layers with hot-melt adhesive. Its ion exchange capacity and the pressure drop with flow rate of water were measured and the adsorption of vanadium (V) ions on the hybrid ion exchanger was evaluated with various process parameters such as pH, initial concentration, and temperature. It was observed that the adsorption kinetics of vanadium (V) ions on the hybrid ion exchanger could be analyzed with pseudo-second-order model.

1. Introduction

Many researchers have studied the treatment of heavy metals such as copper, lead, and cadmium in wastewater due to the regulation of effluent water in industry. Especially, vanadium (V) having strong toxicity is widely used in various industries such as ceramic, glass, and textile. Thus, its recovery in wastewater has lately become a subject of special interest among heavy metals.

The adsorption of vanadium (V) on various adsorbents is considered to be an important issue. The adsorbent materials with bead and flake-type such as chitosan [1–5], chemically modified silica [6–10], and aluminum-pillared bentonite [11] have been widely used for the removal of vanadium ions from aqueous solution.

Removal of metal ions using ion exchange fiber has recently been investigated to overcome the disadvantages of ion exchange bead, which has a good selectivity on metal ions, but also have processing limitations such as high bed pressure drop and long treatment time [12–18]. However, ion exchange fibers with high adsorption rate of metal ions have low packing density, which leads in a decrease in the ion exchange capacity. The binding method using solution-type adhesives has good bonding strength. However, the active functional groups on ion exchanger are covered by the adhesive to be finally inactivated. In the present work, the hot-melt spraying method was applied for binding with ion exchange fiber and ion exchanger resin. Therefore, we present herein new type of ion exchanger, which was formed to be combined commercial ion exchange bead with ion exchange fiber by hot-melt bonding method. The ion exchange fiber to be used in this study was synthesized by radiation-induced polymerization method [14].

The sorption process of the vanadium (V) can be considered to be controlled by three steps: (1) transfer of the vanadium (V) from the bulk solution to adsorbent surface, (2) intraparticle diffusion from the surface to the pores of the adsorbent, and (3) adsorption of the vanadium (V) on the active sites. Many researchers have considered that the rate controlling step is the mass transfer resistances in steps (1) and (2) because step (3) is generally assumed to be rapid with respect to steps (1) and (2) and is neglected in any kinetic analysis [3,19]. However, the recent work has demonstrated that the adsorption process is transport-limited in initial process, but become dominant chemical adsorption in the process [20].

The present paper has addressed the use of a hybrid ion exchanger (HIE) which consists of ion exchange fiber and resin combined with hot-melting adhesive for the effective adsorption of vanadium (V). In view of the above, the present work investigated the pressure drop with various flow rates, ion exchange capacity with bead layers, and the kinetics of vanadium (V) ions onto HIE in a batch experiments. The influence of initial solution concentration, pH, and solution temperature is also observed.

* Corresponding author. Tel.: +82 42 821 5687; fax: +82 42 821 5681.
E-mail address: tshwang@cnu.ac.kr (T.-S. Hwang).

0304-3894/$ – see front matter © 2008 Elsevier B.V. All rights reserved.
doi:10.1016/j.jhazmat.2008.11.032

2. Adsorption kinetics of vanadium (V) on hybrid ion exchange

2.1. Elovich model

Elovich model describe the adsorptive capacity with time as following equation [21]:

$$\frac{dq_t}{dt} = r_a \exp(-r_d q_t) \tag{1}$$

where q_t (mg/g) is the sorption capacity of the hybrid ion exchanger at time t and r_a (mg/g min) is the initial sorption rate and r_d (g/mg) is the desorption rate during any one experiment. Eq. (5) is obtained with Eq. (2) and boundary conditions [22].

$$r_a r_d t \rangle\rangle 1 \tag{2}$$

$$\text{Boundary conditions}: t = 0, \quad q_t = 0 \tag{3}$$

$$t = t, \quad q_t = q_t \tag{4}$$

$$q_t = \frac{1}{r_d}\ln(r_a r_d) + \frac{1}{r_d}\ln(t) \tag{5}$$

2.2. Pseudo-second-order model

Pseudo-second-order model has been widely used to analyze the adsorption of heavy metal ions on different ion exchangers [23,24]. The adsorption of metal ions on any adsorbent is represented as following equation:

$$\frac{dq_t}{dt} = k(q_e - q_t)^2 \tag{6}$$

where q_t (mg/g) is the adsorption of vanadium (V) on the ion exchanger at time t and q_e (mg/g) is the equilibrium adsorption of vanadium (V) on the ion exchanger at infinite time and k (g/mg min) is the reaction rate constant. Integrating Eq. (6) using boundary conditions (3) and (4), Eq. (7) can be obtained as an arranged form:

$$\frac{t}{q_t} = \frac{1}{h} + \frac{1}{q_e}t \tag{7}$$

At t approaches 0, the initial sorption rate, h (mg/g min), is defined as following:

$$h = kq_e^2 \tag{8}$$

For minimizing the error during the linear least-square method, a trial-and-error method was used to calculate r_a and r_d in Eq. (5), q_e and k in Eq. (7) using Excel solver add-in function [23].

3. Flow resistance through hybrid ion exchange

The flow resistance through any fibrous filter is mainly affected by fiber diameter (d_f), flow stream viscosity (μ), face velocity (U_0), filter thickness (L_f), and dimensionless fiber drag, $f(\alpha)$ which is a function of the packing density of filter media [26]:

$$\Delta P_f = \frac{\mu U_0 L_f}{d_f^2} f(\alpha) \tag{9}$$

where c is the solid volume fraction which has been published with various equations by many researchers [27–29]. Meanwhile, the pressure drop of the resin packed bed is determined by resin diameter (d_p), fluid stream density (ρ), face velocity, bed length (L_b), void fraction of the bed (ε), dynamic viscosity (μ), and friction factor ($f(r)$) [30]:

$$\Delta P_r = \frac{\rho U_0^2 L_b}{d_p}\left(\frac{1-\varepsilon}{\varepsilon^3}\right) f(r) \tag{10}$$

where $f(r)$ is the friction factor for the packed bed and is related with Re as following equation:

$$f(r) = \frac{150}{Re} + 1.75 \tag{11}$$

$$Re = \frac{d_p U_0 \rho}{(1-\varepsilon)\mu} \tag{12}$$

As can be shown in Eqs. (9) and (10), the factors to affect on the pressure drop of the fiber and the resin are its packing density and diameter.

4. Experimental

4.1. Preparation of hybrid ion exchanger

The substrate of ion exchange fiber was used a bicomponent polyolefin fiber (PONF) having polyethylene sheath and polypropylene core provided by Namyang Nonwoven Co. and its basic properties were shown in Table 1. The PONF-g-GMA copolymer was synthesized by irradiation method and was functionalized by the amination reaction which makes it an anionic ion exchanger. And, Amberlite IRA-96 (Fluka Co.) was used as ion exchange resin. These two different types of ion exchangers were bound with each other using hot-melt adhesive and their configurations were shown in Fig. 1. The detail procedure was reported in the previous report [25].

4.2. Ion exchange capacity and flow resistance

The HIE was immersed and stirred in 0.1 M NaOH solution for 24 h. The replaced HCl was titrated with 0.1 M NaOH solution. Ion exchange capacity (IEC) was determined as following:

$$\text{IEC (meg/g)} = \frac{N_{\text{NaOH}}\left(V_{\text{NaOH}}/1000\right) N_{\text{HCl}}\left(V_{\text{NaOH}}/V_{\text{ion exchanger}}\right)\left(V_{\text{NaOH}}/1000\right)}{\text{mass of dry ion exchanger}} \times 100 \tag{13}$$

where N_{NaOH} and N_{HCl} are the normality and V_{NaOH} and V_{HCl} are total volume of used NaOH and HCl for the titration, respectively.

For measuring the flow resistance of HIE, the sample was put into the column with 50 mm inner diameter and pure water was fed into the column with constant flow rate by centrifugal pump, and then the pressure drop was recorded. The flow rate to be used was in range of 0.58–1.91 m/s.

4.3. Adsorption of vanadium

The adsorption kinetic study was carried out by mixing 0.15 g of HIE with 50 mL of vanadium oxide (V_2O_5) solution, which was placed in conical flask with 100 mL volume. The effects of the process parameters were observed with pH (3, 5 and 7), initial concentration (0.25, 0.50 and 1.00 mM) and temperature (283, 293 and 313 K). The pH was controlled and maintained at the reference value by adding 0.1 M nitric acid. The solution was agitated by a mixer. The concentration of vanadium in the solution was obtained by 2 mL in each solution and analyzed by Inductively Coupled Plasma

Table 1
Basic properties of PE/PP bicomponent fiber.

Composition	PE/PP
Ratio	50:50
Fiber diameter (μm)	20
Elongation (%)	30
Specific tension (g/d)	5.5

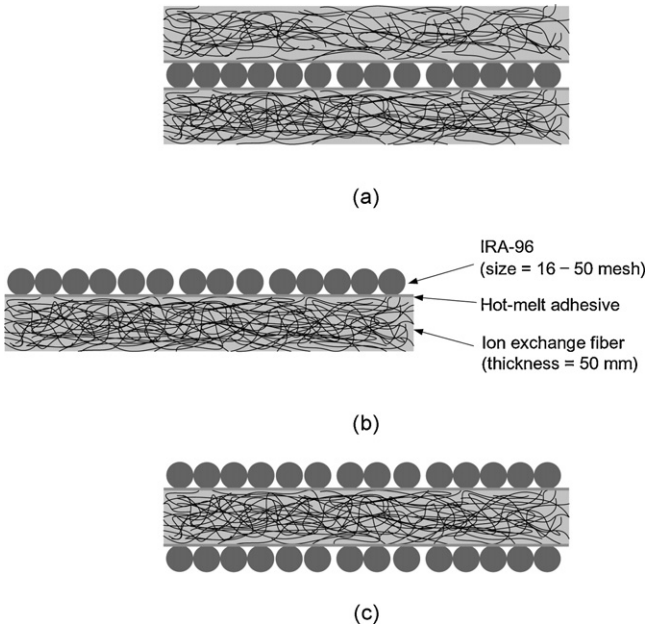

Fig. 1. Configurations of the hybrid ion exchanger with ion exchange fibers and resins: (a) fiber:resin = 2:1, (b) fiber:resin = 1:1, and (c) fiber:resin = 1:2.

(ICP, Thermo Jarrel Ahs Co., Atomscom 25 model). The adsorbed concentration of vanadium on the ion exchanger was calculated at any time t by a following mass balance equation:

$$q_t = \frac{(C_0 - C_t)V}{m} \quad (14)$$

where C_0 and C_t (mM) are the initial concentration of vanadium (V) ion and the vanadium (V) ion concentration at any time t (min) in the solution, and V (mL) is the solution volume and m (g) is the weight of ion exchanger to be used.

5. Results and discussion

5.1. Ion exchange capacity

Fig. 2 shows the cross-sectional structures of the HIE with two kinds of the ratio of fiber and resin ion exchangers obtained from SEM analysis. As shown in Fig. 2, the HIE had a hot-melt layer to be formed on the interface between fibers and beads, which provided a good linkage with different-type ion exchangers. The range of bead size is 510–1580 μm and the average fiber diameter is about 20 μm. Moreover, the small gaps between fibers and the additional hot-melt spraying layer prevented the beads from invading among the fibers. Using these properties, it can be minimized to be loss of the adsorption capability of the hybrid ion exchanger by bonding process. In addition, the combination of the fiber layer and bead layer can be choose freely, and then the ion exchange capacity and the pressure drop of the HIE can be designed on the purpose of the targeted performance. Table 2 shows the ion exchange capacity of HIE with various ratios of bead and fiber. The ion exchange capacities of the fiber and the bead are 2.4 and 2.2, respectively and that of the HIE is in the range between two types of the ion exchangers. And, the ion exchange capacity of the HIE decreased with increasing the ratio of the bead layer, and eventually approached to the ion exchange capacity of the bead. There is no stiff change with hot-melt spraying and stacked bead layers. The ion exchange capacity of HIE with various bead layers illustrates the effectiveness of hot-melt binding in the combination of the ion exchangers with bead and fiber.

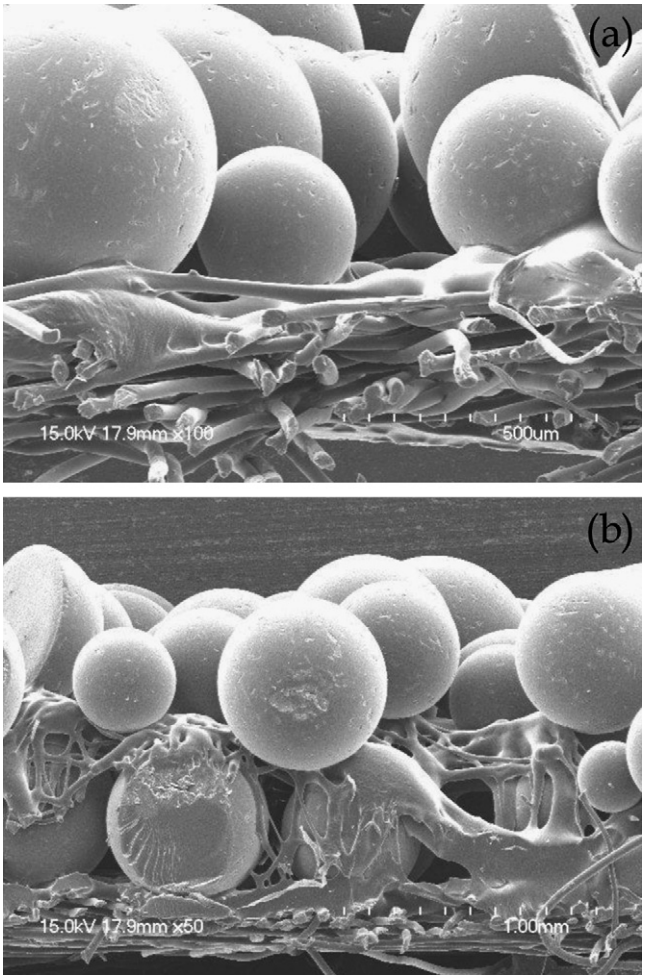

Fig. 2. Scanning electron microscopy images of hybrid ion exchanger: (a) fiber:resin = 1:1 and (b) fiber:resin = 1:2.

5.2. Flow resistance of ion exchanger

Fig. 3 shows the effect the flow rates on the flow resistance of the HIE with various its layers. As previously mentioned, the most advantage of the ion exchange fiber is very low-pressure drop compared to the ion exchange resin. The pressure drop of the ion exchange fiber is 1.7–7.7 mmH_2O with flow rate in the range of 0.58–1.91 m/s, which has 4.53 of the slope. Meanwhile, the slope of the pressure drop of HIE was steeply increased to 11.53, 28.71, 33.04, and 32.69 from 1 layer to 4 layer of the resin, respectively. And the pressure drop of HIE was mainly affected by the resin above 2 layer. The fiber itself and 1 layer-bead hybrid ion exchanger have lower slope with the flow rate than that of more layer-bead HIE. Therefore, hybrid ion exchanger can be designed with the stack of 1 layer-bead HIE in consideration of the ion exchange capacity and the flow rate to be used in the process.

Table 2
Ion exchange capacity of hybrid ion exchanger.

Ion exchanger	Weight of fiber (g)	Weight of bead (g)	Ion exchange capacity (meq/g)
Fiber	5	–	2.40
Fiber + 1 layer resin	5	10	2.31
Fiber + 2 layer resin	5	20	2.27
Fiber + 3 layer resin	5	30	2.25
Fiber + 4 layer resin	5	40	2.23
Resin	–	10	2.20

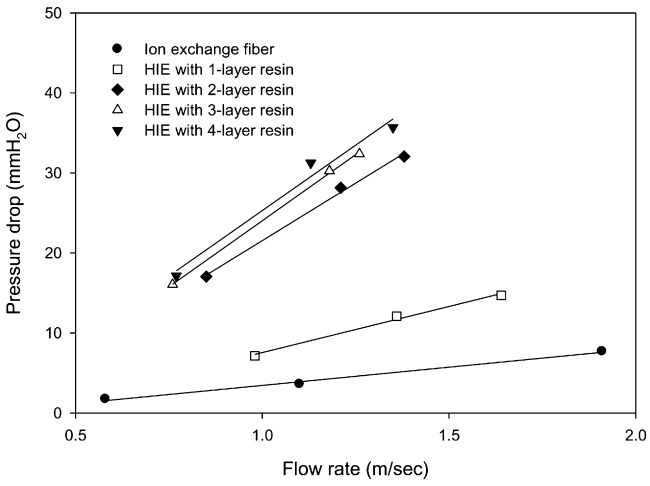

Fig. 3. Flow resistance through the hybrid ion exchanger with flow rates.

The ion exchange fiber typically has low-pressure drop due to their very low packing density (in general, 0.01–0.3) regardless of its fine diameter compared to the ion exchange resin [31]. The ion exchange capacity of the fiber per unit volume, however, is smaller than that of the resin. Therefore, the HIE to be developed in this study is a good alternative to compensate the disadvantages of two different types of the ion exchanger: fiber and resin.

5.3. Kinetic models for the hybrid ion exchanger

Fig. 4 shows the plot of the adsorption of vanadium (V) ions on HIE based on Elovich model and pseudo-second-order model. Based on Eq. (5), Elovich model was shown as the plot between q_t and t, which is used to calculate two rate constants by nonlinear trial-and-error method. As shown in Fig. 4(a), however, the experimental data for all kinds of HIE to be plotted based on Elovich model did not agree well with the correlation coefficient, r^2, in range of 0.773–0.956.

The equilibrium adsorption capacity and the rate constant based on pseudo-second-order model were obtained by trial-and-error method in Excel solver add-in function using the nonlinear data of q_t and t [23]. Fig. 4(b) showed the adsorption of vanadium (V) ions was agreed with the pseudo-second-order model with the correlation coefficient, r^2, in range of 0.908–0.997 and this means this kinetic model can be well describes the experimental data. The reaction rate to be calculated based on this kinetic model is given in Table 3. Due to its better fitting with all kinds of HIEs, the pseudo-second-order model can be considered as more proper kinetic model for the adsorption of vanadium (V) ions on the HIE than Elovich model. The amount of vanadium (V) ions adsorbed at the equilibrium time increased from 16.57 to 25.58, and the rate constant of the pseudo-second-order model decreased from 36.51×10^{-4} to 1.03×10^{-4} with increasing the ratio of the resin. While the reaction rate of the ion exchange fiber is 35 times faster than the ion exchange resin, the equilibrium adsorption capacity of the fiber is 65% of that of the resin. The reaction rate between the ion exchanger and metal ions was generally ignored for analyzing the adsorption mechanism because it is very faster than the diffusion rate of metal ions. However, when the diffusion reaches steady state, total adsorption of metal ions on the ion exchanger is controlled by the reaction rate between the functional group of the ion exchanger and metal ions [20].

In this study, for the HIE to be consisted of resins and fibers, pseudo-second-order model is considered to explain the adsorption behavior of vanadium (V) very well.

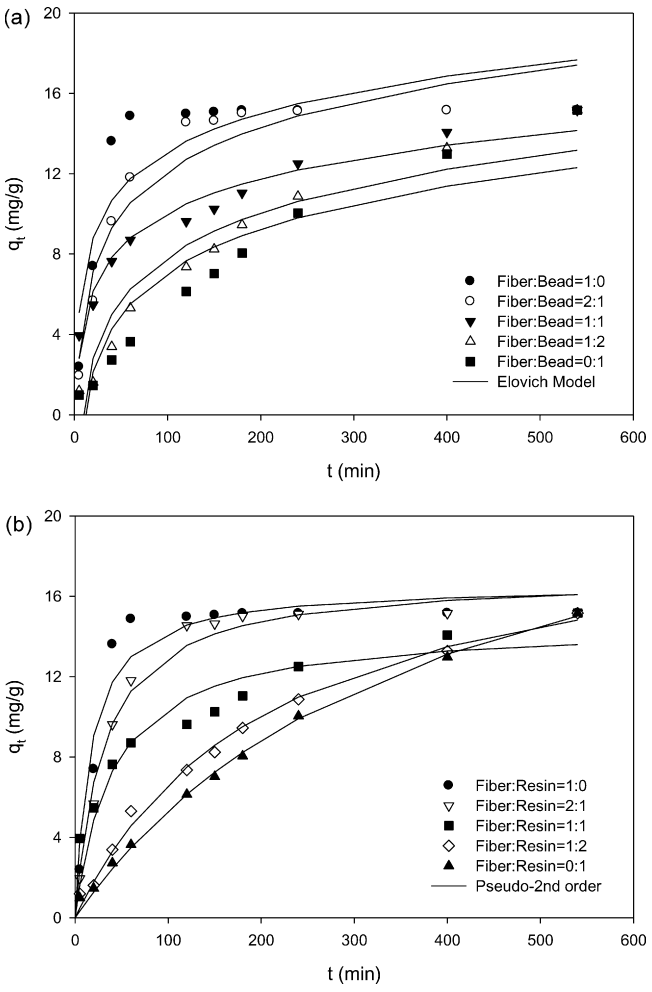

Fig. 4. Adsorption kinetic models for vanadium (V) ions on hybrid ion exchanger based on (a) Elovich model and (b) pseudo-second-order model at temperature of 40 °C, pH 5 and initial concentration of 0.25 mM.

5.4. Effect of process parameters

The effect of pH on the adsorption of vanadium (V) ions onto HIE was studied in range of pH 3–7. The hydrolysis of vanadium (V) and the proton exchange property of the HIE are affected by pH, and therefore, the adsorption rate of vanadium (V) on the HIE is varied depending on that of the solution. As shown in Fig. 5, the fitting lines based on pseudo-second-order model showed the agreement with the experimental data, which has the correlation coefficient, r^2, between 0.727 and 0.951 in pH range of 3–7. The total charges of ion exchangers such as alluminum-pillared bentonite and modified chitosan are positive and the hydrolyzed species of vanadium (V) were dominantly formed in low pH and eventually, the adsorption of vanadium (V) ions on those ion exchangers was enhanced [3,11]. Increasing pH results in decreasing the adsorption

Table 3
Parameters for pseudo-second-order model.

Fiber:resin	Parameter			
	q_e (mg/g)	k (g/mg min)	h (mg/g min)	r^2
1:0	16.57	36.51×10^{-4}	1.00	0.908
2:1	16.99	19.38×10^{-4}	0.56	0.976
1:1	14.60	17.13×10^{-4}	0.37	0.915
1:2	20.55	2.33×10^{-4}	0.10	0.994
0:1	25.58	1.03×10^{-4}	0.07	0.997

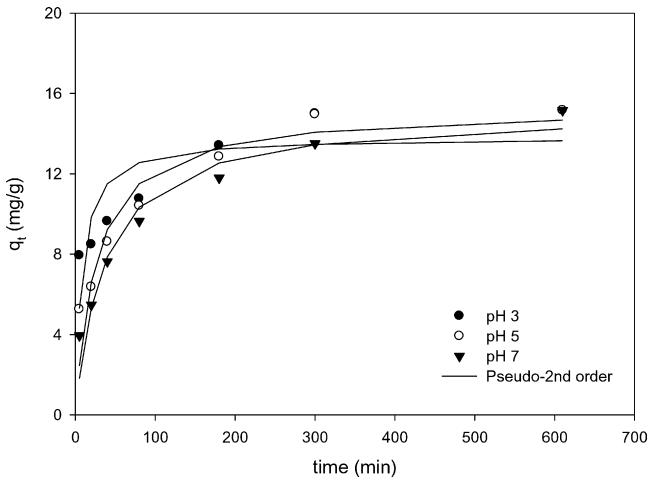

Fig. 5. Effect of solution pH on the adsorption of vanadium (V) ions on hybrid ion exchanger (fiber:bead = 1:1) at temperature of 40 °C and initial concentration of 0.25 mM.

rate of vanadium (V). The ion exchange resin used in this study is an anionic exchanger with amine functional group and with operating pH between 0 and 7. And, the ion exchange fiber also has the same functional group with the resin. Vanadium (V) forms different hydrolyzed species with pH and solution concentration. The principle-hydrolyzed species formed are followed with pH used in this study [32,33]:

$$10VO_2^+ + 8H_2O \leftrightarrow V_{10}O_{26}(OH)_2^{4-} + 14H^+ \quad pK_1 = 6.74 \tag{15}$$

$$V_{10}O_{26}(OH)_2^{4-} \leftrightarrow H^+ + V_{10}O_{27}(OH)^{5-} \quad pK_2 = 3.6 \tag{16}$$

$$V_{10}O_{27}(OH)^{5-} \leftrightarrow H^+ + V_{10}O_{28}^{6-} \quad pK_3 = 5.8 \tag{17}$$

When pH is increased 3–7, VO_2^+ is diminished and other three forms such as $V_{10}O_{26}(OH)_2^{4-}$, $V_{10}O_{27}(OH)^{5-}$, and $V_{10}O_{28}^{6-}$ coexists in the solution. Due to these ions, the adsorption capacity of vanadium (V) on the HIE was increased from 13.83 to 15.10 with increasing pH and the optimum pH value is 5 for the sorption of vanadium (V). This result agrees with previous studies that the optimum pH range for sorption of vanadium (V) ions is between 3 and 8 [4,7]. The reaction rate of vanadium (V) ions with the functional group of HIE, however, became slow with increasing solution pH. In the case of a sorbent with low porosity, its sorption kinetics is affected by metal ion concentration in the boundary layer [3]. As shown from reaction rate and the correlation coefficient, r^2, in Fig. 6 and Table 4, the deviation between experimental data and pseudo-second-order model in low pH exists due to lower concentration of hydrolyzed species in low pH than that in high pH.

Table 4
Parameters for pseudo-second-order model with various process factors.

Factor	Constant			
	q_e (mg/g)	k (g/mg min)	h (mg/g min)	r^2
pH				
3	13.83	89.66×10^{-4}	1.72	0.727
5	15.31	24.76×10^{-4}	0.58	0.918
7	15.10	18.02×10^{-4}	0.41	0.951
Initial concentration (mM)				
0.25	15.49	14.95×10^{-4}	0.36	0.939
0.50	33.24	2.76×10^{-4}	0.31	0.994
1.00	46.72	4.36×10^{-4}	0.95	0.993
Temperature (K)				
283	15.01	12.94×10^{-4}	0.29	0.984
293	15.10	18.02×10^{-4}	0.41	0.951
313	15.22	30.09×10^{-4}	0.70	0.994

The influence of initial concentration on the adsorption of vanadium (V) ions was examined over the initial concentration range of 0.25–1.00 mM. Based on Eq. (9), the plot of q_t versus t with three different initial concentrations was shown in Fig. 5. The result demonstrates a highly significant linear relationship between q_t and t within 0.25–1.0 mM initial concentration with the correlation coefficient, r^2, in the range of 0.939–0.993. The values of the rate constant (K) was varied from 14.95×10^{-4} to 2.76×10^{-4} in keeping with initial concentrations. These high correlation between q_t and t suggests that the chemical interaction between the vanadium (V) ions to be adsorbed through the solution and the amino groups on the HIE dominated the adsorption attachment. Increasing the vanadium (V) concentration in the solution seems to reduce the diffusion of vanadium (V) ions in the boundary layer and to enhance the diffusion in the ion exchanger [3]. Therefore, the equilibrium adsorption is increased from 15.49 to 46.72 in range of 0.25–1.0 mM of the initial concentration of vanadium (V) ions in the solution. And the ion exchanger with low porosity is affected by the concentration of the metal ions and the size of the ion exchanger due to low diffusion rate of the metal ion through the film region and neglecting the intraparticle diffusion [3].

Effect of the solution temperature on vanadium (V) adsorption onto the HIE was studied under the temperature between 283 and

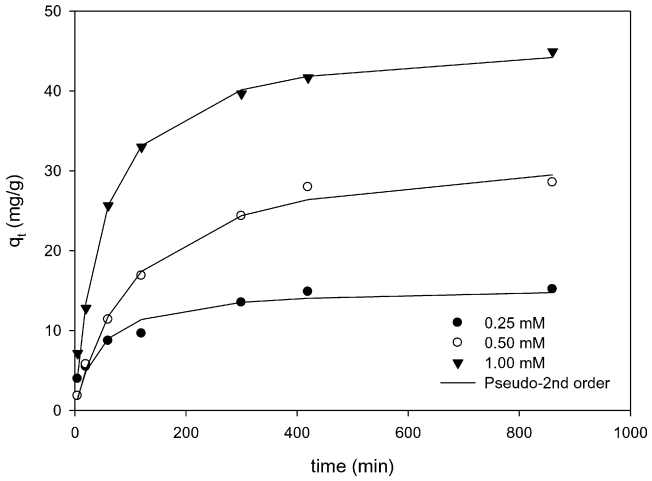

Fig. 6. Effect of initial concentration on the adsorption of vanadium (V) ions on hybrid ion exchanger (fiber:bead = 1:1) at temperature of 40 °C and pH 5.

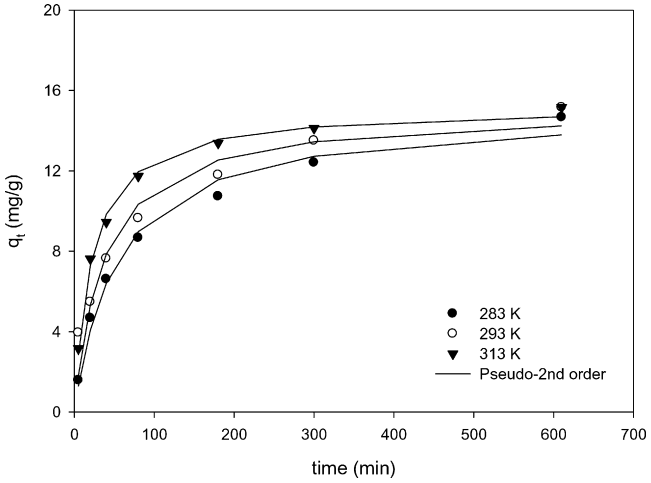

Fig. 7. Effect of temperature on the adsorption of vanadium (V) ions on hybrid ion exchanger (fiber:bead = 1:1) at pH 5 and initial concentration of 0.25 mM.

313 K and was showed in Fig. 7 in which the correlation coefficient is between 0.951 and 0.994. As shown in Table 4, the equilibrium adsorption capacity is slightly increased from 15.01 to 15.22 and the rate constant is increased above twice from 12.94×10^{-4} to 30.09×10^{-4}. Solution temperature affect to electroselectivity reaction, ion salvation formation of ion pairs, and association and formation of complexes between vanadium (V) ions and the ion exchanger. And, the diffusion rate of the ion through film boundary region becomes faster with increasing temperature, and therefore, reaction rate is also increased [11].

6. Conclusion

The sorption of vanadium (V) ions could be analyzed by Elovich model and pseudo-second-order model on hybrid ion exchanger which was developed by hot-melt spraying between ion exchange resin and the fibers with amine functional group and the resin. The bonding method used in this study little affected on the ion exchange capacity of hybrid ion exchanger. The effects of the system parameters such as solution pH, initial concentration, and temperature were also discussed. In the case of our hybrid ion exchanger, pseudo-second-order model described the adsorption of vanadium (V) ions better than Elovich model. This research is expected to be applicable on the analysis and optimization of the adsorption of various heavy metals on the ion exchanger with various combinations.

Acknowledgements

This study was supported by a grant from the industry-academic cooperation project, Small and Medium Business Administration (SMBA), Republic of Korea (Project Number: 00262920108).

References

[1] S.H. Qian, H.Y. Wang, G.Q. Huang, S.B. Mo, W. Wei, Studies of adsorption properties of crosslinked chitosan for vanadium(V), tungsten(VI), Journal of Applied Polymer Science 92 (2004) 1584–1588.
[2] J. Guzman, I. Saucedo, R. Navarro, J. Revilla, E. Guibal, Vanadium interactions with chitosan: influence of polymer protonation and metal speciation, Langmuir 18 (2002) 1567–1573.
[3] M. Jansson-Charrier, E. Guibal, J. Roussy, B. Delanghe, P. LeCloirec, Vanadium (IV) sorption by chitosan: kinetics and equilibrium, Water Research 30 (1996) 465–475.
[4] E. Guibal, I. Saucedo, M. Janssoncharrier, B. Delanghe, P. Lecloirec, Uranium and vanadium sorption by chitosan and derivatives, Water Science and Technology 30 (1994) 183–190.
[5] R. Navarro, J. Guzman, I. Saucedo, J. Revilla, E. Guibal, Recovery of metal ions by chitosan: sorption mechanisms and influence of metal speciation, Macromolecular Bioscience 3 (2003) 552–561.
[6] C.E. Dogan, U. Koklu, Sorption and preconcentration of vanadium, chromium, manganese, and lead on silica gel modified with (3-mercaptopropyl) trimethoxysilane, Instrumentation Science & Technology 34 (2006) 359–366.
[7] K. Pyrzynska, T. Wierzbicki, Sorption behavior of vanadium on silica gel modified with tetrakis(4-carboxyphenyl)porphyrin, Analytical Sciences 21 (2005) 951–954.
[8] C. Ekinci, U. Koklu, Determination of vanadium, manganese, silver and lead by graphite furnace atomic absorption spectrometry after preconcentration on silica-gel modified with 3-aminopropyltriethoxysilane, Spectrochimica Acta Part B-Atomic Spectroscopy 55 (2000) 1491–1495.
[9] V.I. Fadeeva, T.I. Tikhomirova, G.V. Kudryavtsev, I.B. Yuferova, Sorption preconcentration, separation, and determination of vanadium(V), Molybdenum(Vi) and tungsten(Vi) using chemically modified silica, Journal of Analytical Chemistry 47 (1992) 341–350.
[10] Z.A. Sadikova, T.I. Tikhomirova, A.V. Lapuk, V.I. Fadeeva, Sorption of vanadium(IV), vanadium(V), and molybdenum(VI) on silica chemically modified with iminodiacetic acid groups, Journal of Analytical Chemistry 52 (1997) 206–208.
[11] D.M. Manohar, B.F. Noeline, T.S. Anirudhan, Removal of vanadium(IV) from aqueous solutions by adsorption process with aluminum-pillared bentonite, Industrial & Engineering Chemistry Research 44 (2005) 6676–6684.
[12] X.P. Liao, W. Tang, R.Q. Zhou, B. Shi, Adsorption of metal anions of vanadium(V) and chromium(VI) on Zr(IV)-impregnated collagen fiber, Adsorption-Journal of the International Adsorption Society 14 (2008) 55–64.
[13] Z.J. Ding, L. Qi, J.Z. Ye, Research on preparation of sheath–core bicomponent composite ion exchange fibers and absorption properties to metal ion, Macromolecular Research 16 (2008) 21–30.
[14] I.H. Cho, K.W. Baek, Y.M. Lim, Y.C. Nho, T.S. Hwang, Synthesis of POF cation exchange fibers using PE coated PP matrix by radiation-induced polymerization and their adsorption properties for heavy metals, Polymer-Korea 31 (2007) 239–246.
[15] V. Kumar, Y.K. Bhardwaj, K.A. Dubey, C.V. Chaudhari, N.K. Goel, J. Biswal, S. Sabharwal, K. Tirumalesh, Electron beam grafted polymer adsorbent for removal of heavy metal ion from aqueous solution, Separation Science and Technology 41 (2006) 3123–3139.
[16] P.A. Kavakli, N. Seko, M. Tamada, O. Guven, Adsorption efficiency of a new adsorbent towards uranium and vanadium ions at low concentrations, Separation Science and Technology 39 (2004) 1631–1643.
[17] A. Jyo, J. Kugara, H. Trobradovic, K. Yamabe, T. Sugo, M. Tamada, T. Kume, Fibrous iminodiacetic acid chelating cation exchangers with a rapid adsorption rate, Industrial & Engineering Chemistry Research 43 (2004) 1599–1607.
[18] N.S. Kwak, T.S. Hwang, S.M. Kim, Y.K. Yang, K.S. Kang, Synthesis of sulfonated PET-g-GMA fine ion-exchange fibers for water treatment by photopolymerization and their adsorption properties for metal ions, Polymer-Korea 28 (2004) 397–403.
[19] K.K.H. Choy, D.C.K. Ko, C.W. Cheung, J.F. Porter, G. McKay, Film and intraparticle mass transfer during the adsorption of metal ions onto bone char, Journal of Colloid and Interface Science 271 (2004) 284–295.
[20] C.X. Liu, R.B. Bai, Preparation of chitosan/cellulose acetate blend hollow fibers for adsorptive performance, Journal of Membrane Science 267 (2005) 68–77.
[21] M.J.D. Low, Kinetics of chemisorption of gases on solids, Chemical Reviews 60 (1960) 267–312.
[22] S.H. Chien, W.R. Clayton, Application of Elovich equation to the kinetics of phosphate release and sorption in soils, Soil Science Society of America Journal 44 (1980) 265–268.
[23] Y.S. Ho, Second-order kinetic model for the sorption of cadmium onto tree fern: a comparison of linear and non-linear methods, Water Research 40 (2006) 119–125.
[24] Y.S. Ho, D.A.J. Wase, C.F. Forster, Batch nickel removal from aqueous-solution by sphagnum moss peat, Water Research 29 (1995) 1327–1332.
[25] K.W. Baek, S.W. Park, Y.C. Nho, T.S. Hwang, Synthesis of high loading PONF-g-GMA anion exchange fiber containing ion exchange resin and their adsorption properties of vanadium, Polymer-Korea 31 (2007) 315–321.
[26] Q. Wang, B. Maze, H.V. Tafreshi, B. Pourdeyhimi, A case study of simulating submicron aerosol filtration via lightweight spun-bonded filter media, Chemical Engineering Science 61 (2006) 4871–4883.
[27] N. Rao, M. Faghri, Computer modeling of aerosol filtration by fibrous filters, Aerosol Science and Technology 8 (1988) 133–156.
[28] H. Okuzaki, T. Takahashi, N. Miyajima, Y. Suzuki, T. Kuwabara, Spontaneous formation of poly(*p*-phenylenevinylene) nanofiber yarns through electrospinning of a precursor, Macromolecules 39 (2006) 4276–4278.
[29] J. Happel, Viscous flow relative to arrays of cylinders, AICHE Journal 5 (1959) 174–177.
[30] S. Ergun, Fluid flow through packed columns, Chemical Engineering Progress 48 (1952) 89–94.
[31] W.C. Hinds, Aerosol Technology: Properties, Behavior, and Measurement of Airborne Particles, 2nd ed., Wiley, New York, 1999.
[32] C.F. Baes Jr., R.E. Mesmer, The Hydrolysis of Cations, Wiley, New York, 1976.
[33] R. Navarro, J. Guzman, I. Saucedo, J. Ravilla, E. Guibal, Recovery of metal ions by chitosan: sorption mechanisms and influence of metal speciation, Macromolecular Bioscience 3 (2003) 552–561.